

Recent Progress in Synchrotron Radiation Spectroscopy and Spectromicroscopy

G. MARGARITONDO^{*, **}, J. ALMEIDA^{*}
and Gelsomina De STASIO^{*, ***}

^{*} *Institut de Physique Appliquée, Ecole Polytechnique Fédérale*

^{**} *Sincrotrone Trieste SCpA*

^{***} *Istituto di Struttura della Materia, Consiglio Nazionale delle Ricerche*

We briefly review some of the latest developments in the field of synchrotron-radiation microscopy and spectromicroscopy. The cases which we specifically discuss include: the first spectromicroscopy experiments at new ultrabright synchrotron sources; some sophisticated applications of spectromicroscopy to neurobiology; the first tests of a novel transmission microscopy technique for soft-x-rays. Finally, we will briefly discuss the progress towards the implementation of spectromicroscopy techniques based on the free electron laser.

1. The Advent of Ultrahigh Brightness

The third generation of synchrotron radiation sources is now reality; specifically, in the soft-x-ray range four new facilities are in operation in Trieste (ELETTRA), Hsinchu-Taiwan (SRRC, Synchrotron Radiation Research Center), Pohang-South Korea (PAL, Pohang Accelerator Laboratory) and Berkeley (ALS, Advanced Light Source) — and Bessy-II in Berlin is under construction.

One common characteristic that distinguishes all of these new facilities from previous synchrotron sources is ultrahigh brightness¹⁻³⁾. Roughly speaking, the brightness is proportional to the emitted flux normalized by the photon beam's geometric dimensions (source size and angular divergence)¹⁻³⁾. Thanks to the improved geometry for the electron beam and to the extensive use of undulators, the brightness of the new sources stands at least two orders of magnitude higher than previous undulator sources at Wisconsin, LURE-Orsay and other facili-

ties — and 4-5 orders of magnitude above the average synchrotron sources used for the overwhelming majority of the present experiments.

This improved performance's cost has been high as far as human, technical and financial resources are concerned. On the other hand, the new performance levels open up tremendous new opportunities for research, and the possibility of implementing experiments which would have been unthinkable until now.

The present review discusses one of the fields which is most likely to take advantage of the new levels of brightness. We are talking about synchrotron x-ray microscopy or the combination of x-ray spectroscopy and microscopy, known as *spectromicroscopy* — the best known version of which is photoelectron spectromicroscopy³⁻¹²⁾.

The need for brightness in microscopy and spectromicroscopy derives from very basic considerations. In virtually all of the photon microscopies

* Institut de Physique Appliquée, Ecole Polytechnique Fédérale CH-1015 Lausanne, Switzerland
Telephone t41 (0) 21-693-44-75
Telefax t41 (0) 21-693-46-66

and spectromicroscopies, one needs to concentrate a large photon flux in a small area by using a focused beam. Consider first the *scanning* photon microscopy techniques (Fig. 1): focusing the photon beam into a small spot is required in this case⁴⁻⁷⁾ to achieve high lateral resolution. Focusing the photon beam is not strictly required but still highly desirable for other approaches — such as those in which the lateral resolution is achieved⁸⁻¹²⁾ by using an electron optical system to process emitted particles, e.g., photoelectrons. In fact, even a partial focusing of the photon beam improves the experimental conditions by increasing the signal

level.

On the other hand, the focusing of a photon beam is governed by a specific version of the phase-space-volume-conservation Liouville theorem⁷⁾. In essence, this makes it impossible to decrease the combination of angular divergence and beam size along a beamline: strong focusing of a beam of limited brightness would imply large angular divergence with a series of technical problems — some of which are essentially insurmountable. The bottom line is that focusing is much easier, and in some cases only possible, if the source has high brightness.

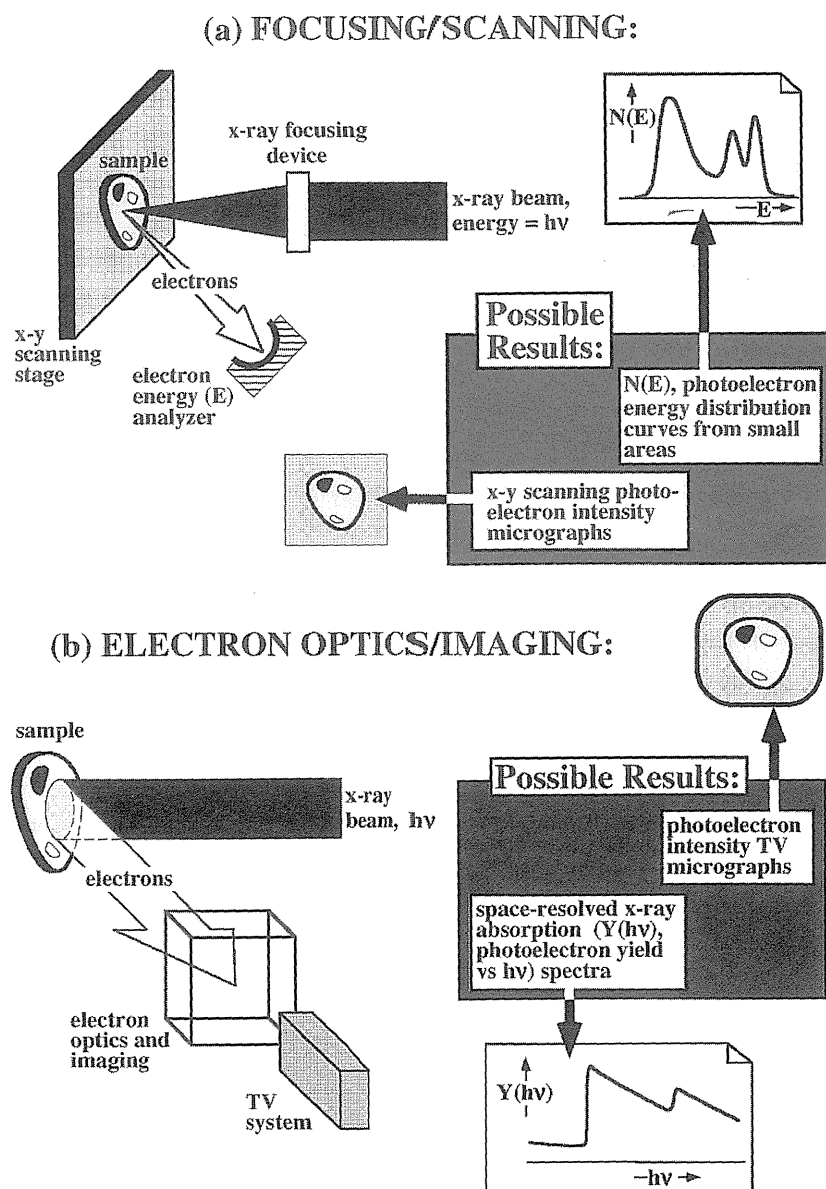


Figure 1. Schematic illustration of the two general classes of synchrotron spectromicroscopy techniques, including some of their possible products. The specific example illustrated here refers to photoelectron spectromicroscopy (Refs. 3-12)

This basic point is well known to the scientific and technical community that has struggled for decades to use synchrotron radiation for microscopy experiments. Not surprisingly, this community was the first to exploit the newly commissioned ultrabright sources, and to perform experiments with them^{13, 14}.

The present review describes some of the relevant recent events in this field. We will not extensively describe the basic features of spectroscopy and spectromicroscopy, since these have been discussed at length by a series of recent reviews³⁻¹². We will try instead to illustrate the present trends in the evolution of this domain, using specific new results. Some of our objectives are: (1) to demonstrate that synchrotron radiation spectroscopy and - above all - spectromicroscopy are no longer techniques under test, but mature and established research tools; (2) to show how this approach is branching into new areas, notably how photoelectron spectromicroscopy is expanding into transmission microscopy¹⁵, and how the general trend towards high lateral resolution is beginning to touch the free electron lasers¹⁶.

2. First Results from the New Facilities

The fact that synchrotron microscopy and spectromicroscopy is no longer a domain under test is primarily due to the very rapid progress in the quality of the instrumentation. We will illustrate this point with one practical example. Figure 2a shows the very first attempt (in 1989-90) to use synchrotron photoelectron microscopy to image a neurobiological specimen¹⁷. Although historically relevant, this image is certainly far from being satisfactory as far as the quality of microscopy are concerned.

Figures 2b and 2c show more recent¹⁴ synchrotron photoelectron spectromicroscopy images from a brain-cell specimen of the same type as Fig. 2a. The quality improvement is quite striking, in particular if one takes into account the relatively short time over which it was achieved. This improvement makes it possible to definitely leave the "testing" stage, and to use these wonderful new techniques for real experiments in the life sciences as well as in materials science — as we discuss later.

The result of Figs. 2b and 2c are a nice example of how techniques in this general family have inaugurated the use of the new ultrabright synchrotron source. These images were produced by Hwu et al.¹⁴ at the recently commissioned SRRC facility in

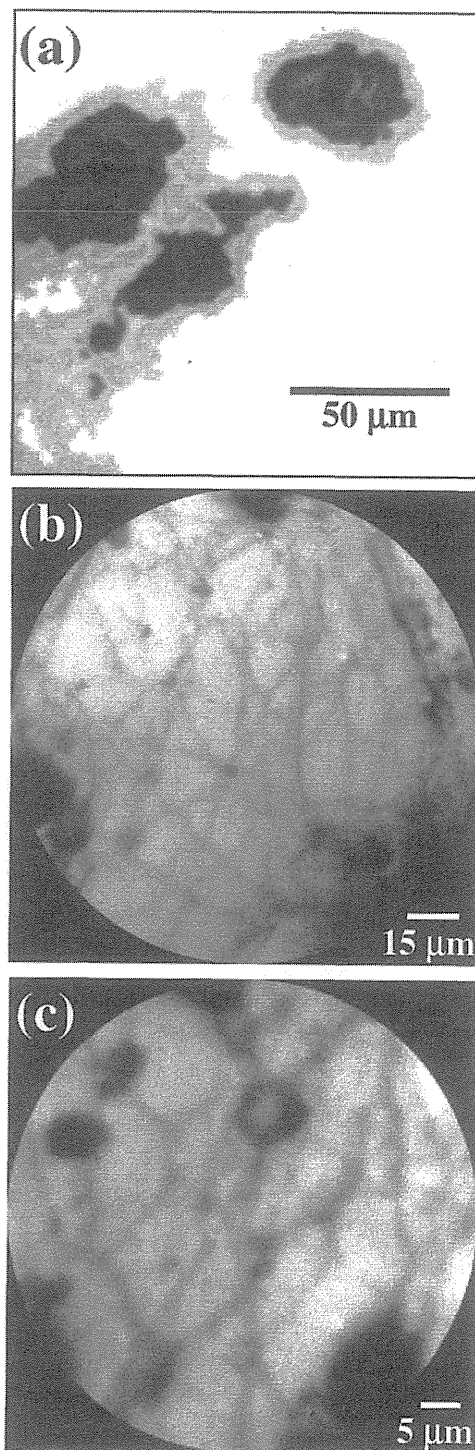


Figure 2. Three different photoelectron spectromicroscopy microimages for brain cell cultures, which illustrate the very rapid progress of this field from the first tests in 1990 (Fig. 2a, from Ref. 17) to recent results (Figs. 2b and 2c) from Ref. 14.

Hsinchu Taiwan; the experiments involved scientists from four different countries, and very quickly produced microimages of excellent quality.

Figures 2b and 2c also give us the opportunity to discuss one of the two basic modes of synchrotron

radiation spectromicroscopy, as illustrated in Fig. 1b — the one in which the spatial resolution is produced by an electron optical system⁸⁻¹². The “spectroscopy” performance of the technique is obtained in this case by scanning the photon energy. The “spectra” are photoelectron yield vs photon energy curves. These have been demonstrated long ago¹⁰ to reproduce the x-ray absorption coefficient of the surface region.

Figure 3 shows another example of this approach, also obtained by Hwu et al.¹⁴ at the Taiwan source, on high-temperature superconducting samples grown by Berger et al.¹⁴. The objective of the experiment was to test the chemical homogeneity of high-quality single crystals of BCSCO, which are specifically grown for sophisticated spectroscopy studies¹⁹.

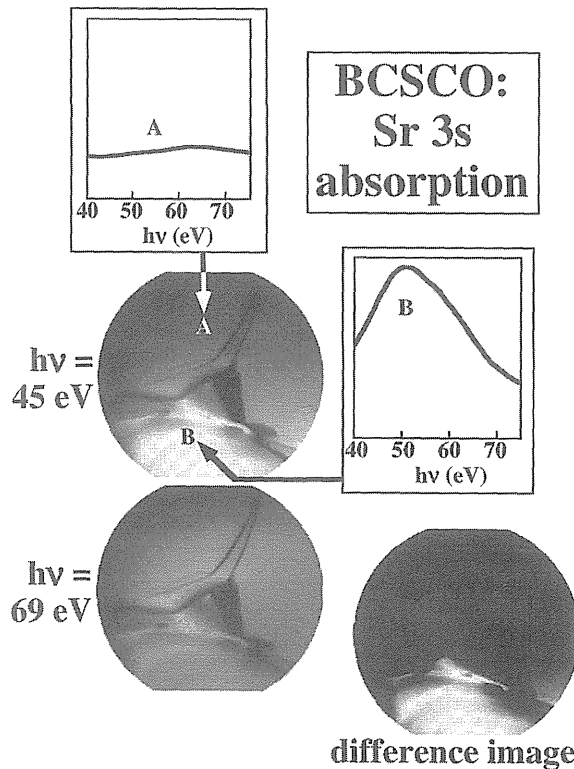


Figure 3. An electron optics-imaging study of the chemical composition of a high-temperature superconducting BCSCO-2212 specimen. We see two micrographs taken at two different photon energies in the spectral range of a Sr x-ray absorption edge, plus their pixel-by-pixel difference. Spatial features that do not depend on $h\nu$ are of topographic origin; in addition, we see an area with $h\nu$ -dependent intensity. A comparison of partial-yield (x-ray absorption) spectra taken inside and outside the area reveals in this latter an excess amount of Sr. The difference image emphasizes the spatial distribution of the excess Sr. The results are from the first spectromicroscopy experiment at the SRRC facility in Hsinchu, Taiwan¹⁴.

We see in the images of Fig. 3 the different dependence of different features on the photon energy. There are features that are almost unchanged as the photon energy is scanned: these are most likely topographic features on the contrary, we see regions whose intensity changes when the photon energy is modified — in this case, scanned across one of the Sr x-ray absorption edges. These regions correspond to areas of anomalous Sr content, probably microprecipitates. Overall, the sample homogeneity was found to be excellent. Nevertheless, the high sensitivity of the spectromicroscopy technique made it possible to find a very small portion of one sample with Sr microprecipitates.

Experiments of this type have also inaugurated another soft-x-ray source of the third generation, the synchrotron ELETTRA in Trieste. The first publishable data were obtained in a world record time: *two weeks* after the first electron injection¹⁵.

Experiments in this class have continued for more than one year on ELETTRA. Quite recently, this approach has been complemented by a second beamline, based on the focusing-scanning technique of Fig. 1a. The beamline (“ESCA Microscopy”) was jointly implemented by the Sincrotrone Trieste SCpA, by the ENIRICERCHÉ company and by King’s College²⁰.

The core of the instrument is its focusing device, a Fresnel zone plate which demagnifies the photon beam to submicron dimensions, delivering up to 10^{10} photons/second in the focusing spot. The synchrotron source in this case is an 81-period undulator with a 56 mm period, covering the range 1000-1500 eV with its first three harmonics. The beamline operates in the spectral domain 200-1200 eV, and the microscope is expected to reach a resolution better than 0.1 micron.

The lateral resolution of the beamline is illustrated²⁰ in Fig. 4, which shows the photoelectron microimage of a test pattern (actually, a portion of a zone plate with zones of decreasing width). One can clearly see zones whose width is 0.1 micron or less.

Figure 5 shows one of the first experiments with the beamline²⁰, a test chemical-contrast image of a gold film on holey carbon. The chemical contrast, corresponding to the “spectroscopic” capabilities of the technique, is obtained in this case by selecting the energy of the detected photoelectrons. The selected energy for Fig. 5 corresponds to Au4f electrons, which reveal the presence of Au.

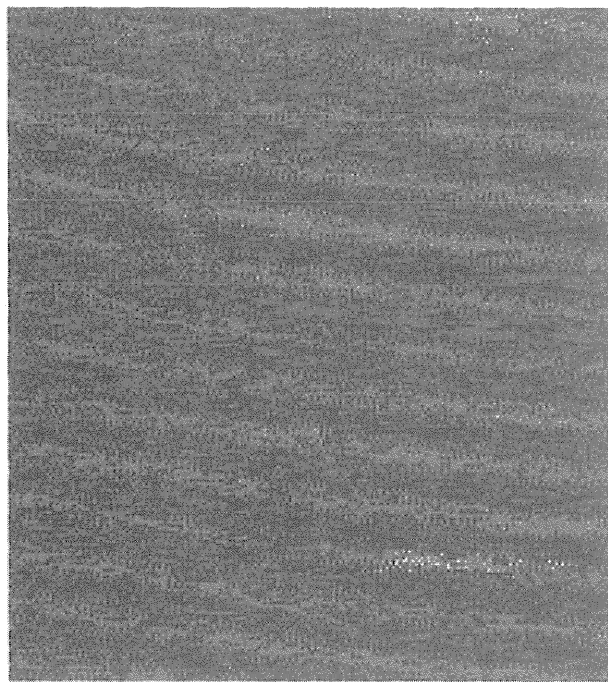
5 μm

Figure 4. First results of the ESCA spectromicroscopy beamline on ELETTRA (from Casalis et al., Ref. 20): $5 \times 5 \mu\text{m}^2$ image of the zones of a $100 \mu\text{m}$ gold amplitude zone plate with line-to-space ratio 1:1 and zone height $\approx 130 \text{ nm}$; the step size was $0.05 \mu\text{m}$.

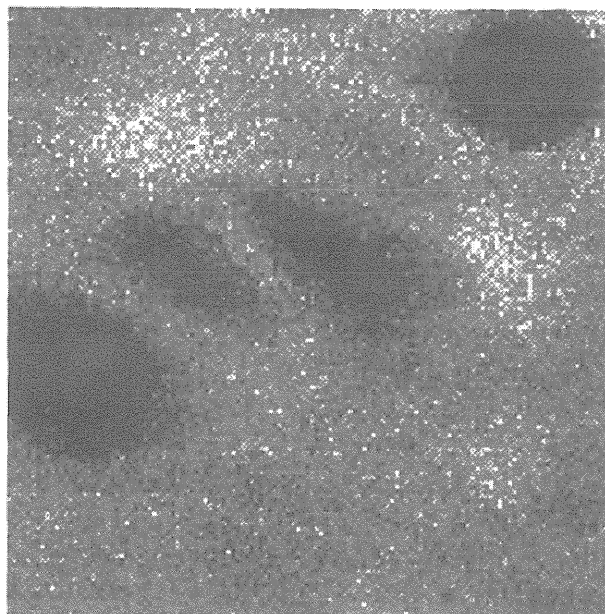
6 μm

Figure 5. More results from the first tests of the ESCA spectromicroscopy beamline of ELETTRA (from Casalis et al., Ref. 20 and M. Kiskinova, unpublished): $6 \times 6 \mu\text{m}^2$ image of a sample consisting of a 15 nm thick gold film over holey carbon. Step size: $0.025 \mu\text{m}$.

3. Spectromicroscopy at a Mature Stage: Neurobiological Studies

The examples of the previous section show how the new ultrabright synchrotron sources have been rapidly begun to support test experiments in microscopy and spectromicroscopy. One should not have the impression, however, that these experimental techniques are still at the "test" stage. On the contrary, they are quite mature, after years of successful development and fine-tuning at the second-generation sources. The advent of the third-generation sources further improves performances that are already quite impressive.

In order to practically illustrate this point, we will present here an example of the use of an electron-optics photoelectron spectromicroscopy technique⁸⁻¹². The example²¹ is only a small portion of an extensive research program⁹⁻¹² on the uptake of toxic metals by neuron systems. The results

discussed here concern the uptake of zinc in different types of rat cerebellar primary cultures, part of which had been exposed to zinc-containing solutions.

The purpose was to study the exposure-stimulated zinc uptake, and specifically the relative role of the cell's membrane (the "surface") vs the cytoplasm (the "bulk"). These experiments, therefore, constitute an extension of one of the standard approaches¹ used by surface to distinguish between "surface" and "bulk" phenomena. The discrimination is possible by comparing results of experimental techniques with and without surface sensitivity. In the present case, the surface-sensitive technique was the XSEM (X-ray Secondary Electron-emission Microscopy) mode of synchrotron apectromicroscopy⁸, and the bulk-sensitive technique was ICP-AES (Inductively-Coupled-Plasma Atomic Emission Spectroscopy)²²⁻²⁴.

The results were quite straightforward: the Zn exposure does not significantly modify the membrane Zn concentration with respect to the physiological levels, whereas it does increase the zinc concentration in the cytoplasm. The same result was obtained for all types of brain cells included in the experiments: glial cells, granule and Purkinje neurons and astrocytes²⁵⁾.

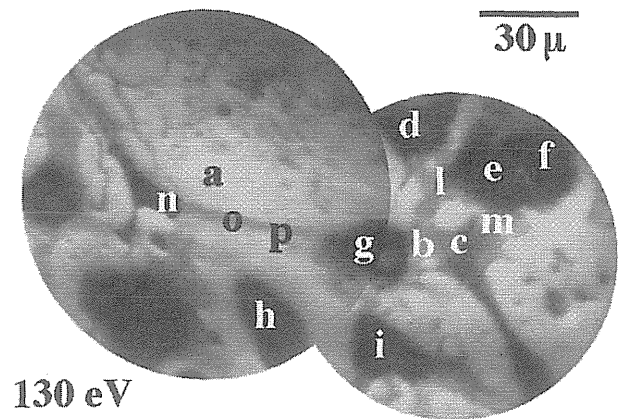
Before commenting of specific results, we note that synchrotron spectromicroscopy can investigate biological specimens without previous coating and labeling, and therefore in a state more similar to the natural one than in most electron microscopies. However, this approach is not feasible for the use of live specimens because of the need of ultrahigh vacuum and therefore of previous dehydration of the sample.

Figure 6 shows an example of spectromicroscopy results: a photoelectron yield microimage for a specific type of cell, together with a series of XSEM spectra taken at different points of the same image. Figure 6 refers to polygonal (type I) glial cells from a culture with a prevailing population of cells of this kind. The bottom part of Fig. 6 shows XSEM spectra taken in the correspondingly labeled microscopic areas of the top part of the same figure. The spectral range in each case includes the Zn3s x-ray absorption edge region. And in fact, signal from that edge is clearly visible in all of the spectra. For comparison, the curve labeled as "a" was taken on the substrate and shows no evidence of zinc. For reference, curve "q" was taken instead on a dried droplet of zinc chloride solution in water.

The data in Figs. 6 were taken on cultures that had been exposed to zinc at the end of the growth period. The main issue, of course, was the possible presence of zinc in the cultures prior to exposure. This issue was addressed by investigating cultures that had not been exposed to zinc, and it was found that zinc is indeed physiologically present in the unexposed cultures.

Did the exposure had any effect at all on the amount of zinc present in the cultures? This second issue was addressed by analyzing the zinc concentration in different cultures after different types of zinc exposures. The results, obtained with the ICP-AES technique, show that the Zn exposure dose increase the overall zinc concentration.

The data point to the following straightforward conclusions: since the exposure dose not signifi-



Zn 3s in glial cells

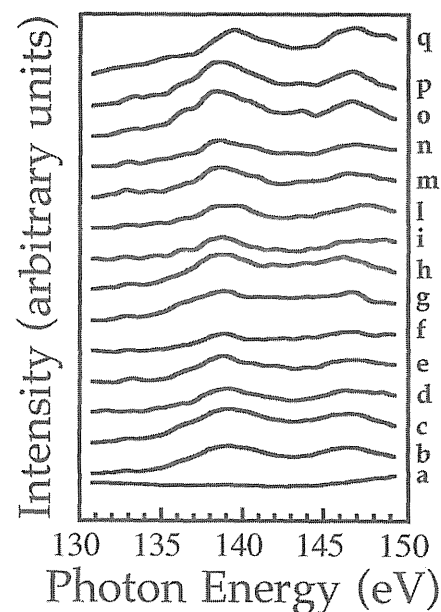


Figure 6. Results for Zn content in brain cell, from Ref. 21. (Top) Combination of two X-ray Secondary Electron Microscopy (XSEM) images of a portion of a culture with prevailing population of glial (type I) cells, after exposure to a 5 mM ZnCl₂ solution for 20 min. The photon energy was 130 eV. The letters identify the microscopic ($\approx 3 \times 3$ micron²) regions in which the spectra of Fig. 1B were taken. (Bottom) XSEM (x-ray absorption) spectra from these regions. The data were background-corrected, normalized and twice-smoothed over five-point sets. Curve (a) refers to a substrate area and is the only one not showing the typical Zn3s absorption threshold lineshape. Curve (q) is a reference spectrum from a dried droplet of a zinc sulfate solution.

ntly affect the zinc concentration in the region probed by spectromicroscopy, the effect of Zn exposure is primarily a "bulk" phenomenon. The "surface" against "bulk" approach of surface science¹⁾ was thus really extended to the life sciences.

Note that photoelectron spectromicroscopy is surface-sensitive because it is based on the detection of mainly secondary photoelectrons^{1,8)}. Their escape depth¹⁾ from a condensed system is not as short as that of primary photoelectrons, which is determined by the mean-free-path for inelastic scattering. Secondary photoelectrons are by definition produced by inelastic scattering events, and their escape depth is determined by the condition that the final energy of a multiple scattering sequence be above the vacuum level. Furthermore, secondary photoelectrons are mostly emitted at low energies, for which even the inelastic-scattering mean-free-path is large.

As a result, the escape depth for secondary photoelectrons is at least one order of magnitude larger than the minimum primary-photoelectron value of 5-10 Å⁷⁾. Even so, a technique like XSEM remains highly surface sensitive, certainly much more than ICP-AES which is not surface sensitive at all. One can estimate the thickness of the region explored by a spectromicroscopy investigation like that of Fig. 6 to be roughly comparable to the thickness of the membrane region plus the membrane proteins and channels.

The data produced by the study indicate, therefore, that Zn is physiologically present, independent of any exposure, both in the membrane and in the cytoplasm. This is not surprising, for example in light of the existence of Zn proteins. The differences between XSEM and ICP-AES data, on the other hand, indicate that the artificial Zn exposures significantly increase only the Zn content in the cytoplasm. This could be either due to a large physiological amount of Zn in the membrane, which is only marginally affected by the exposures, or to a more effective mechanism for exposure-caused uptake in the cytoplasm — or else to a combination of both effects.

The nature and the level of sophistication that synchrotron spectromicroscopy has reached. Many other examples could be cited, including very extensive studies of lateral variations of the parameters of solid surfaces and interfaces, and many cases of investigation of chemical inhomogeneities.

4. New Directions: Transmission Microscopy

The know-how and the instrumentation developed for synchrotron spectromicroscopy can find interesting uses in other, related domains. A recent example¹⁵⁾ of this cross fertilization is the use of

XSEM-related instrumentation for a novel approach to soft-x-ray *transmission* spectromicroscopy with synchrotron radiation. This approach was based on an electron imaging technique rather than on a scanning approach.

The technique consists¹⁵⁾ of converting the transmitted x-rays into photoelectrons with a photocathode, which are subsequently electron optically processed by an XSEM producing submicron-resolution images. The approach was practically and successfully tested by imaging silicon microstructures on a silicon nitride membrane. Images of very good quality were obtained¹⁵⁾, with high contrast and submicron lateral resolution. The intensity contrast could be modified and controlled by changing the photon energy through the absorption edges of the different chemical components of the specimen. Specifically, the contrast between silicon-related features and the silicon nitride membrane was modified by scanning the photon energy through the corresponding Si2p edges.

This last result emphasizes one advantage of this approach: the possibility to work at different photon energies over a wide spectral range, and therefore to move from x-ray transmission microscopy to spectromicroscopy. The spectromicroscopy energy resolution depends only on the photon optics of the synchrotron beamline, both the photon energy range and the energy resolution can be varied. The high signal level makes it possible to perform experiments with real-time imaging.

Figure 7 shows¹⁵⁾ a schematic diagram of the experimental system. The x-rays transmitted through the specimen stimulated the emission of photoelectrons from the photocathode, which consisted of a 50 Å evaporated Au coating on the Si nitride membrane. The photoelectrons were then electron optically processed by the XSEM, which basically consists of an objective lens followed by an aperture stop and by a projective lens⁸⁾. The photocathode coating was kept at a negative voltage bias of several kV and the first element of the objective lens was at ground.

After the XSEM optics, the photoelectron beam was intensified by a double microchannel plate and reached a phosphor screen, producing a visible image viewed and captured by a video system. The video signal was then sent to a computer for acquisition and storage.

With the same apparatus, it is also possible to take x-ray transmission curves from preselected mi-

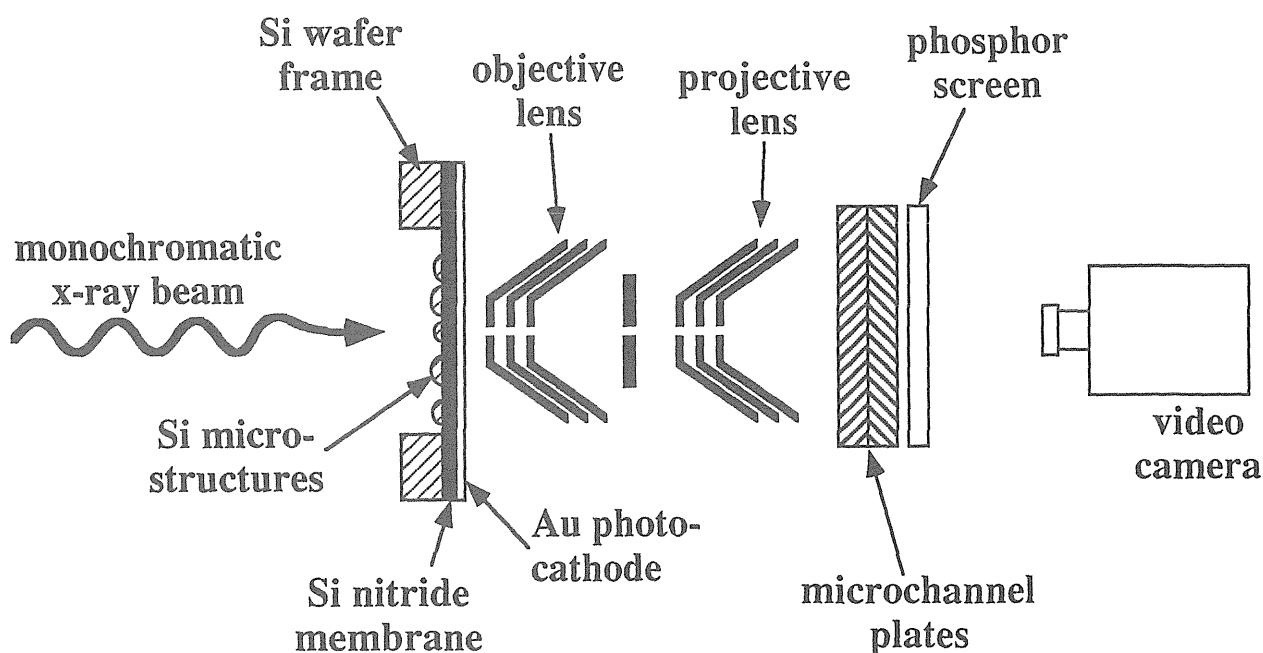


Figure 7. Schematic diagram of the approach to x-ray transmission spectromicroscopy which is reported in Ref. 15.

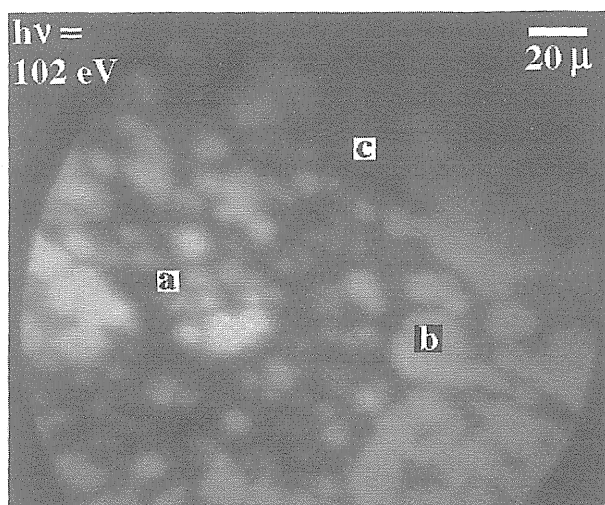


Figure 8. First transmission spectromicroscopy results (from Ref. 15) of the approach illustrated in Fig. 7: X-ray transmission micrograph showing silicon microstructures structures (dark areas) over a silicon nitride membrane. The photon energy was 102 eV, intermediate between the Si2p edges of silicon and silicon nitride. Intensity vs photon energy curves were taken in the areas labeled as a, b and c (see Fig. 3). No image processing was used to enhance the contrast or otherwise modify the data.

croscopic areas of the specimen, by scanning the photon energy and measuring the local image intensity. This is directly related to the transmitted photon intensity which reaches the photocathode and stimulates the emission of (mostly secondary)

electrons.

Figure 8 shows¹⁵⁾ a typical transmission micrograph, obtained at a photon energy of 102 eV. At this photon energy, silicon nitride is transparent whereas silicon absorbs. In the image, the absorbing silicon microfeatures appear as dark areas. These microfeatures are due to silicon residuals left after the chemical etching on the silicon nitride membrane.

Figure 9 demonstrates the spectromicroscopic capabilities of the approach¹⁵⁾. We see three transmission curves as a function of photon energy, simultaneously taken in the areas labeled as a, b and c in Fig. 9. Note that all three curves exhibit features corresponding to the silicon and silicon nitride Si2p absorption edges (100 and 104 eV). In curves a and c, which correspond to silicon microstructures in Fig. 8, we see a strong silicon edge and a relatively weak silicon nitride edge. On the contrary, the silicon nitride edge is most prominent in curve b, which indeed corresponds to a bright area of Fig. 8.

Note that no image processing was done on the data of Fig. 8. Even so, one can appreciate a very high contrast in spite of the small sample thickness, which demonstrates the apparatus' high sensitivity to chemical differences. This is of fundamental importance in life-science applications such as the microchemical analysis of thin tissue sections —

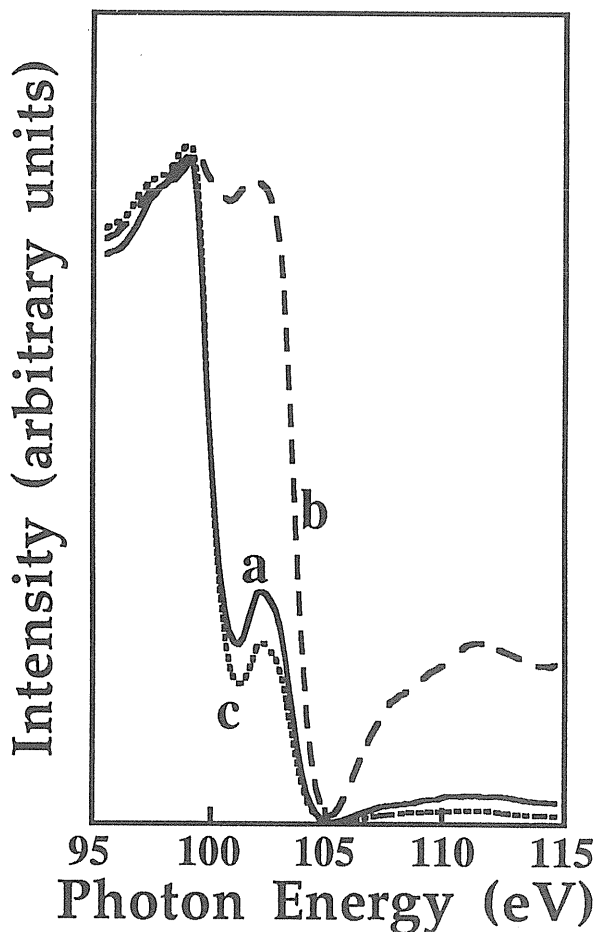


Figure 9. Spectroscopic results from the same experiments of Fig. 8 (Ref. 15): transmitted X-ray intensity as a function of photon energy simultaneously taken in the three areas a, b and c of Fig. 8. The curves were normalized and corrected for the background to obtain two isosbestic points at 99.2 and 105 eV.

which is affected by charging problems in other spectromicroscopies.

5. New Directions. Free Electron Lasers

The general domain of synchrotron microscopy and spectromicroscopy might be extended in the near future to another type of synchrotron-related photon sources: the free electron lasers (FEL's)^{16,26}. Of course, the spectral domain of these sources is no longer (at least at the present time) in the soft-x-ray range, but in the infrared¹⁻³. Nevertheless, many of the concepts developed for soft-x-ray spectroscopy and spectromicroscopy could be easily transferred to FEL-based techniques.

We would like to discuss in this section a specific example of this evolution¹⁶. For some time, FEL's have been used in the so-called internal photoemission (IPE) approach for accurate

measurements for the parameters of "buried" solid interfaces²⁶. An effort is underway by Almeida et al.¹⁶ to implement the same FEL experiments with high lateral resolution.

This effort is based on a combination of internal photoemission and nearfield optics. A first successful test was obtained on Pt-GaP: topographic and non-topographic phenomena were revealed, in particular recombination rate variations and small lateral changes of the Schottky barrier height.

In essence, this technique consists¹⁶ of measuring the photocurrent induced in the interface under investigation by an external photon source — in the most advanced cases, an FEL. Interface energy barriers are derived from thresholds in the photocurrent vs photon energy spectra. Information on the recombination rates is also provided by the photocurrent intensity. The space-averaged version of this technique has been extensively used^{26,27}, including a version based on the FEL²⁸ — but no laterally-resolved version had been previously implemented.

High lateral resolution was achieved by illuminating the sample with a small light spot, based on the SNOM (scanning near-field optics microscope) technique²⁹. Figure 10 shows the experimental setup¹⁶. The light source was a tunable DC Ti-Sapphire laser or a solid state laser diode (fixed photon energy at 1.518 eV). The Ti-Sapphire laser provided tunable light in the interval 1.319-1.53 eV. The overall photon energy resolution was ≈ 1 meV, as derived from full width at half maximum of luminescence lines in test samples.

The light beam was chopper-modulated and split in two; one part was detected with a Si avalanche photodiode, the other focused over the metal-covered side of the sample (see below). The tip of the optical fiber was stretched and aluminum-coated to concentrate the light beam into a 50 nm wide pinhole. Piezoelectric translators implemented the vertical approach up to the near-field condition, and the X-Y scanning over a rectangular area of size ranging from 8-30 μ m.

Photocurrent microimages were obtained by detecting the photocurrent signal while scanning the beam over the sample. The photocurrent was revealed with a standard lock-in technique. Topographic images were obtained by measuring the shear-force signal with a synchronous detection including a piezoelectric oscillator and a lock-in amplifier²⁹.

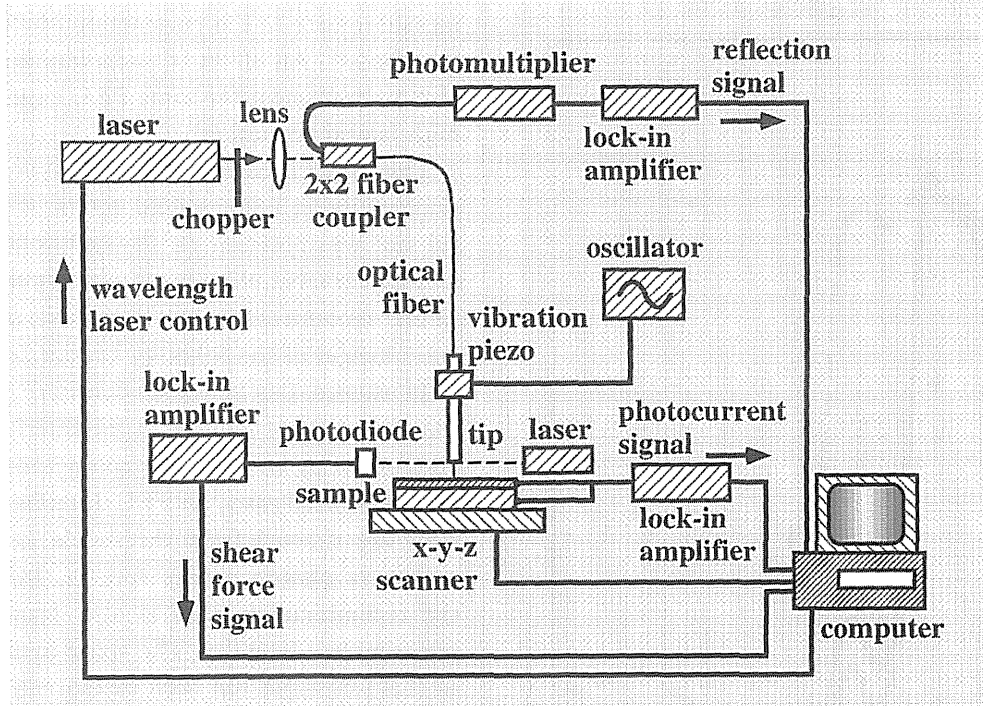


Figure 10. Experimental setup which is under development for free electron laser internal photoemission spectroscopy (see Almeida et al., Ref. 16).

The samples studied in the first test experiment were obtained by electron gun evaporation of Pt on n-type GaP(001). Figure 11 shows typical microimages taken at the photon energy of 1.518 eV (laser diode source). In Fig. 11a, we see the topographic image over a $16 \times 16 \mu\text{m}^2$ area. The analyzed region presents lateral topographic variations on the scale of less than $1 \mu\text{m}$.

A comparison of Figs. 11a and of the photocurrent-intensity image in Fig. 11b shows no one-to-one correspondence between their features: the feature in the marked square is present for both figures, whereas those emphasized by the arrows are only seen in Fig. 11b. Consider, first, the feature in $6 \times 6 \mu\text{m}$ marked square: since it is seen in Fig. 11a, this feature must be of topographic origin.

Now consider the features marked by arrows in Fig. 11b, which are not present in Fig. 11a and therefore cannot have topographic origin. The main non-topographic cause of the IPE intensity inhomogeneities are the local fluctuations in the electron-hole recombination rate.

The same approach is also capable to locally explore the interface energy barriers — Schottky barrier heights in the first tests. Very accurate ($\pm 1 \text{ meV}$) measurements of lateral barrier height variations have been demonstrated. This extends the microscopic-scale applications of FEL-based measu-

SNOM images

$$h\nu = 1.512 \text{ eV}$$

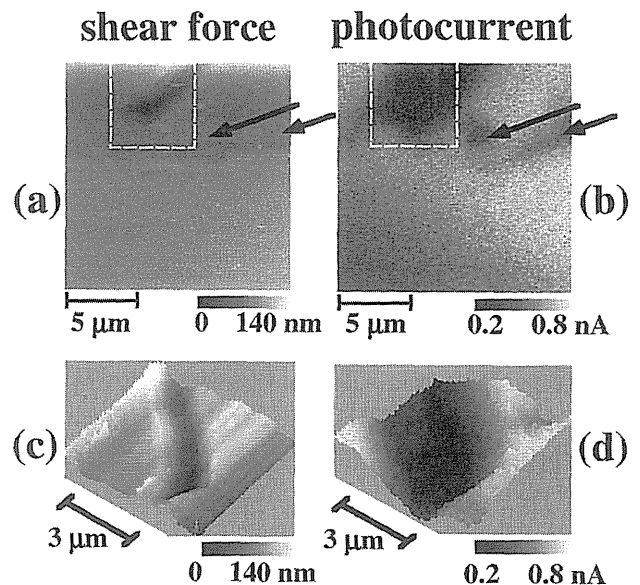


Figure 11. Results of the first tests of the apparatus of Fig. 10, with conventional sources (data from Ref. 16). (a) Shear-force topography and (b) corresponding photocurrent microimage of a $16 \times 16 \mu\text{m}$ in constant distance mode. White pixels on the image are due to “jumps” of the tip. (c) and (d) Enlargement of the $6 \times 6 \mu\text{m}$ marked squares (rotated of 45°) in Figs 11a and 11b. The images show three dimensional reconstructions. The width of the “dark” zone in the photocurrent image is ≈ 1.5 times larger than the corresponding defect.

rements of solid interfaces.

6. Concluding Remarks

The few recent examples discussed in the previous sections cannot, of course, exhaust a field that is in very rapid development. With the availability of additional ultrabright sources, more scientists will be involved in research of this type, and their creativity will undoubtedly multiply the domains of application of synchrotron microscopy and spectromicroscopy. We hope and trust that our short review will convey our enthusiasm to as many colleagues as possible, especially those of the younger generations.

We would like to conclude our remarks with a warning and with a hope. The warning³⁰⁾ is that ultrabright synchrotron radiation cannot be used as a brute-force solutions to the problems of spectromicroscopy (or of any other field). The specific issue here is that spectromicroscopy intrinsically operates in a 3-dimensional space, with one energy coordinate for spectroscopy and two space coordinates for microscopy. This means³⁰⁾ that the typical data set increases in size with a third power law with respect to spectroscopy. And it also implies that mistakes in data-taking strategy that are marginal in the case of spectroscopy could become disastrous for spectromicroscopy.

This problem was recently analyzed³⁰⁾, with the following conclusions: in most cases there exist an optimum compromise between resolution (energy and space) and signal-to-noise ratio. "Optimum" means that the compromise maximizes the extractable information content from the data. Any deviation from the optimum conditions results in a waste of time, i.e., of (expensive) synchrotron beamtime. We thus invite all practitioners of this domain to carefully consider the analysis of Ref. 30.

The warning also leads us to the "hope" message. Basically, the same analysis of Ref. 30 demonstrated that - as one could expect from intuition - any increase in the source brightness also increases the information content of a spectromicroscopy data set (if all other conditions are left unchanged). This confirms the importance of the advent of the third-generation sources. Furthermore, third-generation machines are not the end of the road as far as brightness is concerned³¹⁾.

One of the main steps towards ultrahigh brightness was the introduction of 2-bend or 3-bend

achromats as cells of the magnet lattice in the new storage ring. This concept is now being extended to more complex multiple-bend achromats: the calculations show that the brightness can be further enhanced by at least one order of magnitude³¹⁾. Furthermore, the new sources³¹⁾ would exhibit full coherence at least up to photon energies in the soft-x-ray domain.

These performances, foreseeable for source to be implemented in the next decade, would constitute a new challenge and - indeed - a new hope. The combination of ultrahigh brightness and full coherence could lead to entirely new concepts in spectroscopy and spectromicroscopy, for which we must be prepared well in advance.

Acknowledgments

The author's own research in spectromicroscopy is performed in cooperation with the authors of Refs. 4,5,8-17,19,21,24,26-28 and 31, and supported directly and/or indirectly by the Fonds National Suisse de la Recherche Scientifique, by the European Community, by the Italian National Research Council, by the US Office of Naval Research, by the US National Science Foundation, by the US Department of Energy, by the Ecole Polytechnique Fédérale de Lausanne and by Sincrotrone Trieste SCpA.

References

- 1) G. Margaritondo: *Introduction to Synchrotron Radiation* (Oxford University Press, New York, 1988).
- 2) G. Margaritondo, *J. Synchr. Rad.* 2, 148 (1995).
- 3) G. Margaritondo, *Riv. Nuovo Cimento* 18, 1 (1995).
- 4) W. Ng, A. K. Ray-Choudhury, S. Liang, S. Singh, H. Solak, J. Welnak, F. Cerrina, G. Margaritondo, J. H. Underwood, J. B. Kortright and R. C. C. Perera, *Nucl. Instrum. Meth.* A347, 422 (1994).
- 5) F. Cerrina, B. Lai, C. Gong, A. Ray-Chaudhuri, G. Margaritondo, M. A. Green, H. Höchst, R. Cole, D. Crossley, S. Collier, J. Underwood, L. J. Brillson and A. Franciosi, *Rev. Sci. Instrum.* 60, 2249 (1989); F. Cerrina, S. Crossley, D. Crossley, C. Gong, J. Guo, R. Hansen, W. Ng, A. Ray-Chaudhuri, G. Margaritondo, J. H. Underwood, R. Perera and J. Kortright, *J. Vac. Sci. Technol.* A8, 2563 (1990); W. Ng, A. K. Ray-Chadhuri, R. K. Cole, S. Crossley, D. Crossley, C. Gong, M. Green, J. Guo, R. W. C. Hansen, F. Cerrina, G. Margaritondo, J. H. Underwood, J. Kortright and R. C. C. Perera, *Phys. Scripta* 41, 758 (1990); C. Capasso, A. K. Ray-Chaudhuri, W. Ng, S. Lianf, R. K. Cole, J. Wallace, F. Cerrina, G. Margaritondo, J. H. Underwood, J. B. Kortright and R. C. C. Perera, *J. Vac. Sci. Technol.*

- A9, 1248 (1991).
- 6) H. Ade, J. Kirz, S. Hulbert, E. Johnson, E. Anderson and D. Kern, *Nucl. Instrum. Methods* **291**, 126 (1990).
 - 7) P. L. King, A. Borg, C. Kin, P. Pianetta, I. Lindau, G. S. Knapp, M. Keenlyside and R. Browning, *Nucl. Instrum. Methods* **291**, 19 (1990).
 - 8) B. P. Tonner and G. R. Harp, *Rev. Sci. Instrum.* **59**, 853 (1998); B. P. Tonner and G. R. Harp, *J. Vac. Sci. Technol.* **7**, 1 (1989), S. F. Koranda, J. Zhang, and B. P. Tonner, *Rev. Sci. Instrum.* **63**, 563 (1992).
 - 9) Gelsomina De Stasio, D. Dunham, B. P. Tonner, Delio Mercanti, M. Teresa Ciotti, Paolo Perfetti, G. Margaritondo, *J. Synchrotron Radiation* **2**, 106 (1995).
 - 10) G. Margaritondo, Gelsomina De Stasio and C. Coluzza, *J. Electron Spectr.* **72**, 281 (1995).
 - 11) Gelsomina De Stasio, Delio Mercanti, M. T. Ciotti, T. C. Droubay, P. Perfetti, G. Margaritondo and B. P. Tonner, *Europhys. Lett.* **28**, 283 (1994).
 - 12) Gelsomina DeStasio, Delio Mercanti, M. T. Ciotti, D. Dunham, T. C. Drouby, B. Tonner, P. Perfetti and G. Margaritondo, *NeuroReport* **5**, 1973 (1994).
 - 13) A. Abrami, D. Alfè, S. Antonini, M. Bernardini, M. Bertolo, C. J. Bocchetta, D. Bulfone, F. Cargnello, F. Daclon, S. Di Fonzo, S. Fontana, A. Galimberti, M. Giannini, W. Jark, A. Massarotti, F. Mazzolini, M. Puglisi, R. Richter, A. Rindi, R. Rosei, C. Rubbia, D. Tommasini, A. Savoia, G. Viani, R. Walker, A. Wrulich, C. Coluzza, Tiziana dell'Orto, F. Gozzo, G. Margaritondo, Gelsomina De Stasio, P. Perfetti, M. Gentili, M. T. Ciotti and D. Mercanti, *Nucl. Instrum. Meth.* **A349**, 609 (1994).
 - 14) Y. Hwu, C. Y. Tung, C. Y. Pieh, S. D. Lee, P. Alméras, F. Gozzo, H. Berger, G. Margaritondo, Gelsomina De Stasio, Delio Mercanti and M. Teresa Ciotti, *Nucl. Instrum. Meth.* (in press).
 - 15) Gelsomina De Stasio, T. Droubay, P. Mural, M. Kohli, N. Setter, P. Perfetti, G. Margaritondo and B. P. Tonner, unpublished.
 - 16) J. Almeida, Tiziana dell'Orto, C. Coluzza, G. Margaritondo, O. Bergossi, M. Spajer and D. Courjon, unpublished.
 - 17) Gelsomina De Stasio, W. Ng, A. K. Ray-Chaudhuri, R. K. Cole, Z. Y. Guo, J. Wallace, G. Margaritondo, F. Cerrina, J. Underwood, R. Perera, J. Kortright, Delio Mercanti and M. Teresa Ciotti, *Nucl. Instrum. Methods* **A294**, 351 (1990).
 - 18) W. Gudat and C. Kunz, *Phys. Rev. Lett.* **29**, 169 (1972).
 - 19) Jian Ma, C. Quitmann, R. J. Kelley, H. Berger, G. Margaritondo and M. Onellion, *Science* **267**, 862 (1995).
 - 20) L. Casalis, W. Jark, M. Kiskinova, D. Lonza, P. Melpignano, D. Morris, R. Rosei, A. Savoia, A. Abrami, C. Fava, P. Furlan, R. Pugliese, D. Vivoda, G. Sandrin, F.-Q. Wei, S. Contarini, L. DeAngelis, C. Gariazzo, N. Minnaja, P. Nataletti and G. Morrison, *Rev. Sci. Instrum.* (in press).
 - 21) Gelsomina De Stasio, S. Pochon, F. G. Lorusso, B. P. Tonner, Delio Mercanti, M. Teresa Ciotti, Nino Oddo, Paolo Galli, P. Perfetti and G. Margaritondo, unpublished.
 - 22) R. M. Barnes, *Chemia Analityczna* **28**, 179 (1983); S. Caroli, E. Coni, A. Alimonti, E. Beccaloni, E. Sabbioni and R. Pietra, *Analisis* **16**, 75 (1988); L. Bourier-Guarin, Y. Mauras, J. L. Trelle and P. Allain, *Trace Elem. Med.* **2**, 88 (1985), C. De Martino, S. Caroli, A. Alimonti, F. Petrucci, G. Citro and A. Nista, *J. Exp. Clin. Cancer Res.* **10**, 1 (1991); A. Alimonti, S. Caroli, L. Musmeci et al, *Sci. Total Environm.* **71**, 495 (1988).
 - 23) E. Sabbioni, G. R. Nicolini, R. Pietra et al., *Biol. Trace. Elem. Res.* **26/27**, 757 (1990).
 - 24) Gelsomina De Stasio, P. Perfetti, N. Oddo, P. Galli, Delio Mercanti, M. Teresa Ciotti, S. F. Koranda, S. Hardcastle, B. P. Tonner and G. Margaritondo, *NeuroReport* **3**, 695 (1992).
 - 25) G. P. Wilkin, G. Levi, S. Johnstone et al., *Dev. Brain Res.* **10**, 265 (1983).
 - 26) J. T. McKinley, R. G. Albridge, A. V. Barnes, G. C. Chen, J. L. Davidson, M. L. Languell, P. L. Polavarapu, J. F. Smith, X. Yang, A. Ueda, N. Tolk, CD, Coluzza, P. A. Baudat, C. Dupuy, F. Gozzo, M. Ilegems, D. Martin, F. Morier-Genoud, A. Rudra, E. Tuncel and G. Margaritondo, *J. Vac. Sci. Technol.* **A12**, 2323 (1994).
 - 27) C. Coluzza, G. Margaritondo, A. Neglia and R. Carluccio, *J. Vac. Sci. Technol.* **A10**, 744 (1992); Tiziana dell'Orto, J. Almeida, C. Coluzza, A. Baldereschi, G. Margaritondo, M. Cantile, S. Yildirim, L. Sorba, and A. Franciosi, *Appl. Phys. Lett.* **64**, 16 (1994).
 - 28) C. Coluzza, E. Tuncel, J. L. Staehli, P. A. Baudat, G. Margaritondo, J. T. McKinley, A. Ueda, A. V. Barnes, R. G. Albridge, N. H. Tolk, D. Martin, F. Morier-Genoud, C. Dupuy, A. Rudra and M. Ilegems, *Phys. Rev. B*, **46**, 19 (1992); J. T. McKinley, R. G. Albridge, A. V. Barnes, A. Ueda, N. H. Tolk, C. Coluzza, F. Gozzo, G. Margaritondo, D. Martin, F. Morier-Genoud, C. Dupuy, A. Rudra and M. Ilegems, *J. Vac. Sci. Technol. B* **11** (4), 1614 (1993).
 - 29) E. Betzig and J. K. Trautmann, *Science*, **2576**, 189-195 (1992); E. Betzig, P. L. Finn and J. S. Wiener, *Appl. Phys. Lett.* **60**, 2484 (1994); S. K. Buratto, J. W. P. Hsu, E. Betzig, J. T. Trautman, R. B. Bylisma, C. C. Bahr and M. J. Cardillo, *Appl. Phys. Lett.* **65**, 21 (1994).
 - 30) G. Margaritondo, *Surface Rev. and Lett.* (in press).
 - 31) H. J. Weyer and G. Margaritondo, *Synchrotron Radiation News* **8**, 19 (1995).